Supporting Information

Customizing Phase Separation in Non-Fullerene-Based Organic Photovoltaics: The Impact of Interfacial Morphology

Ling Hong,*[‡a,c] Jiacheng Gong,[‡d] Shihao Chen,[‡c,e] Shengtian Zhu,[c] Zhiyuan Yang,[c] Nan Zheng,[c] Yuanqing Bai,[c] Zhibin Li,[c] Hui Li,[c] Xin Zhou,[d] Yixin Xie,[c] Yungui Li,*[d] Chunchen Liu,*[c] Yufei Zhong*[a,b]

[a]*School of Materials Science and Engineering, NingboTech University, No. 1 South Qianhu Road, Ningbo, 315100, P. R. China. E-mail: hongry@nbt.edu.cn; yufei.zhong@nit.zju.edu.cn*
[b]*Ningbo Global Innovation Center, Zhejiang University, No. 1 South Qianhu Road, Ningbo, 315100, P. R. China*
[c]*Institute of Polymer Optoelectronic Materials and Devices, State Key Laboratory of Luminescent Materials and Devices, South China University of Technology, Guangzhou, 510640, P. R. China. E-mail: mscliu@scut.edu.cn*
[d]*Max Planck Institute for Polymer Research, Ackermannweg 10, Mainz, 55128, Germany. E-mail: yungui.li@mpip-mainz.mpg.de*
[e]*Kingfa Sci.&Tech. Co.,Ltd. No. 88 Kangyuan Road, Shanghai, 201714, P. R. China*
† Electronic supplementary information (ESI) available.
‡ L. Hong, J. Gong and S. Chen contributed equally to this work.

Keywords: organic photovoltaics; morphology optimization; asymmetric side-chains; charge dynamics; non-fullerene acceptors

1. Materials and synthesis

1.1 Materials

D18 and Y6-BO were purchased from Solarmer Energy, Inc. 2PCAz was purchased from Tokyo Chemical Industry (TCI) Co., LTD. All solvents and materials were commercially available and used without further purification.

1.2 Synthesis

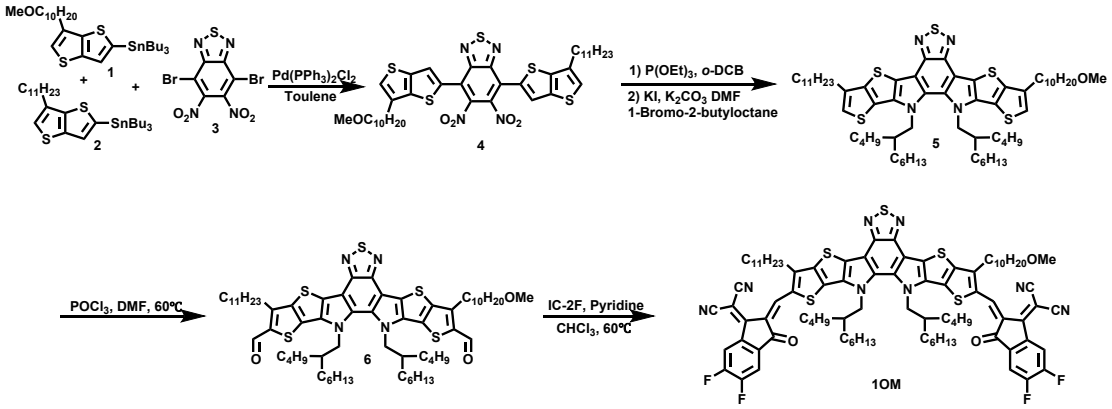

Scheme S1. Synthetic routes of 1OM.

Synthesis of 4-(6-(10-methoxydecyl)thieno[3,2-b]thiophen-2-yl)-5,6-dinitro-()7-(6-undecylthieno[3,2-b]thiophen-2-yl)benzo[c][1,2,5]thiadiazole (4): Compound 1 (3.6 g, 6.0 mmol), compound 2 (3.5 g, 6.0 mmol), compound 3 (1.92 g, 5.0 mmol), and $Pd(PPh_3)Cl_2$ (0.17 g, 0.24 mmol) were dissolved in dry toluene (50 mL), and the reaction mixture was stirred at 80°C under a nitrogen atmosphere overnight. After completion, as monitored by TLC, the mixture was cooled to room temperature and concentrated *in vacuo*. The crude residue was purified by column chromatography on silica gel, eluting with a gradient of dichloromethane in petroleum ether, to afford compound 4 as a red solid (1.53 g, 37% yield).

Synthesis of 12,13-bis(2-butyloctyl)-3-(10-methoxydecyl)-9-undecyl-12,13-dihydro-[1,2,5]thiadiazolo[3,4-e]thieno[2'',3'':4',5']thieno[2',3':4,5]pyrrolo[3,2-g]thieno[2',3':4,5]thieno[3,2-b]indole (5): Compound 4 (2.48 g, 3.0 mmol) and triethyl phosphate (25 mL) were dissolved in *o*-dichlorobenzene (*o*-DCB, 10 mL) under a nitrogen atmosphere. The reaction mixture was heated at 180°C overnight. Upon completion, the mixture was cooled to room temperature and partitioned between water and dichloromethane. The aqueous phase was extracted with dichloromethane, and the combined organic layers were dried over anhydrous Na_2SO_4, filtered, and concentrated *in vacuo*. The resulting red residue was transferred to a three-necked round-bottom flask.

To this, 1-bromo-2-butyloctane (1.24 g, 5.0 mmol), potassium hydroxide (1.00 g, 17.8 mmol), and DMF (30 mL) were added. The mixture was degassed with argon for 15 min and then heated at 80°C under an argon atmosphere for 18 h. After cooling, the reaction was diluted with water and extracted with ethyl acetate. The combined organic extracts were washed with water, dried over anhydrous $MgSO_4$, filtered, and concentrated under reduced pressure. Purification by column chromatography on silica gel, eluting with dichloromethane/petroleum ether, afforded the product as a red solid (1.32 g, 40% yield).

Synthesis of 12,13-bis(2-butyloctyl)-3-(10-methoxydecyl)-9-undecyl-12,13-dihydro-[1,2,5]thiadiazolo[3,4-e]thieno[2'',3'':4',5']thieno[2',3':4,5]pyrrolo[3,2-g]thieno[2',3':4,5]thieno[3,2-b]indole-2,10-dicarbaldehyde (6): Under a nitrogen atmosphere, $POCl_3$ (1.2 g, 8.0 mmol) was slowly added to dry DMF (50 mL) in a two-necked flask. The mixture was stirred at room temperature for 0.5 h, after which a solution of compound 5 (660 mg, 0.60 mmol) in dry CH_2Cl_2 (20 mL) was added dropwise. The resulting reaction mixture was stirred at 60°C for 12 h. Upon completion, the mixture was slowly poured into a saturated aqueous $NaHCO_3$ solution (150 mL) and extracted with ethyl acetate. The combined organic layers were washed with saturated aqueous NaCl, dried over anhydrous Na_2SO_4, filtered, and concentrated under reduced pressure. Purification by column chromatography on silica gel, eluting with a gradient of ethyl acetate in petroleum ether, afforded compound 6 as an orange solid (486 mg, 70% yield).

Synthesis of 2,2'-((2Z,2'Z)-((12,13-bis(2-butyloctyl)-3-(10-methoxydecyl)-9-undecyl-12,13-dihydro-[1,2,5]thiadiazolo[3,4-e]thieno[2'',3'':4',5']thieno[2',3':4,5]pyrrolo[3,2-g]thieno[2',3':4,5]thieno[3,2-b]indole-2,10-diyl)bis(methaneylylidene))bis(5,6-difluoro-3-oxo-2,3-dihydro-1H-indene-2,1-diylidene))dimalononitrile (1OM): To a two-necked flask charged with compound 6 (347 mg, 0.30 mmol) under a nitrogen atmosphere, 2-(5,6-difluoro-3-oxo-2,3-dihydro-1H-inden-1-ylidene)malononitrile (207 mg, 0.90 mmol), $CHCl_3$ (30 mL), and pyridine (1 mL) were added sequentially. The reaction mixture was stirred at 60°C for 12 h. After completion, as monitored by TLC, the solvent was removed under reduced pressure. The residue was purified by column chromatography on silica gel, eluting with dichloromethane/methanol, to afford the desired product 1OM as a dark solid (275 mg, 58% yield). ^{1}H NMR (400 MHz, Chloroform-*d*) δ 9.17 (s, 2H), 8.57 (dd, *J* = 10.0, 6.4 Hz, 2H), 7.70 (t, *J* = 7.3 Hz, 2H), 4.87 – 4.66 (m, 4H), 3.42 – 3.28 (m, 5H), 3.24 (t, *J* = 8.0 Hz, 4H), 2.12 (s, 2H), 1.87 (q, *J* = 7.9 Hz, 4H), 1.51 (d, *J* = 7.5 Hz, 4H), 1.42 – 0.60 (m, 73H). ^{13}C NMR (101 MHz, Chloroform-*d*) δ 186.11, 158.81, 153.87, 147.49, 145.18, 137.69, 136.66, 136.03, 135.23, 134.52, 134.18, 133.28,

119.95, 115.07, 114.97, 114.57, 113.58, 112.52, 72.97, 68.70, 58.54, 55.73, 39.22, 31.93, 31.60, 31.24, 30.51, 30.39, 29.84, 29.67, 29.63, 29.59, 29.53, 29.49, 29.46, 29.41, 29.35, 28.10, 27.90, 26.15, 25.45, 25.25, 22.87, 22.82, 22.70, 22.48, 14.13, 14.03, 13.80, 13.76.

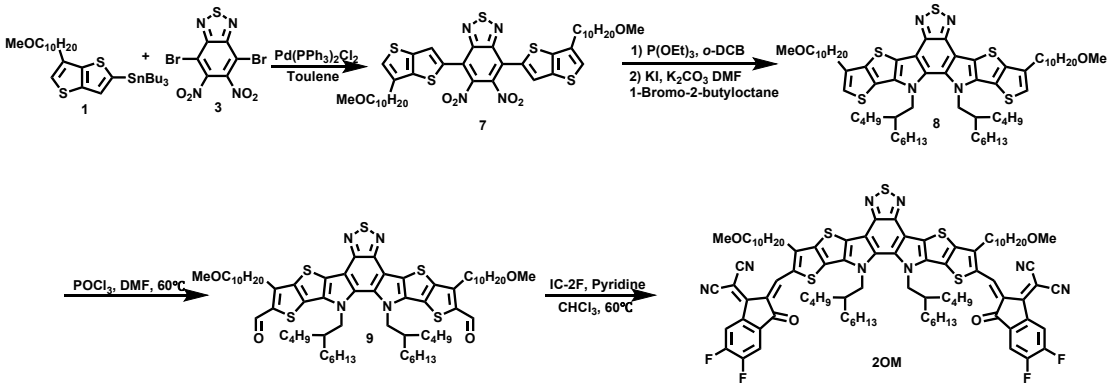

Scheme S2. Synthetic routes of 2OM.

Synthesis of 4,7-bis(6-(10-methoxydecyl)thieno[3,2-b]thiophen-2-yl)-5,6-dinitrobenzo[c][1,2,5]thiadiazole (7): Compound 1 (7.2 g, 12 mmol), compound 3 (1.92 g, 5.0 mmol), and $Pd(PPh_3)Cl_2$ (0.17 g, 0.24 mmol) were dissolved in dry toluene (50 mL) and stirred at 80°C under a nitrogen atmosphere overnight. Upon completion, the reaction mixture was allowed to cool to room temperature and concentrated *in vacuo*. The crude product was purified by column chromatography on silica gel, eluting with a dichloromethane/petroleum ether gradient, to afford compound 7 as a red solid (2.61 g, 62% yield).

Synthesis of 12,13-bis(2-butyloctyl)-3,9-bis(10-methoxydecyl)-12,13-dihydro-[1,2,5]thiadiazolo[3,4-e]thieno[2'',3'':4',5']thieno[2',3':4,5]pyrrolo[3,2-g]thieno[2',3':4,5]thieno[3,2-b]indole (8): Compound 7 (2.53 g, 3.0 mmol) and triethyl phosphate (25 mL) were dissolved in *o*-DCB (10 mL) under a nitrogen atmosphere. The reaction mixture was heated at 180°C overnight. After completion, the mixture was cooled to room temperature and partitioned between water and dichloromethane. The aqueous phase was extracted with dichloromethane, and the combined organic layers were dried over anhydrous Na_2SO_4, filtered, and concentrated *in vacuo*. The resulting red residue was transferred to a three-necked round-bottom flask. To this, 1-bromo-2-butyloctane (1.24 g, 5.0 mmol), potassium hydroxide (1.00 g, 17.8 mmol), and DMF (30 mL) were added. The mixture was degassed with argon for 15 min and then stirred at 80°C under an argon atmosphere for 18 h. Upon completion, the reaction was cooled, diluted with water, and extracted with ethyl acetate. The combined organic extracts were washed with water, dried over anhydrous $MgSO_4$, filtered, and concentrated under

reduced pressure. Purification by column chromatography on silica gel, eluting with dichloromethane/petroleum ether, afforded compound 8 as a red solid (1.47 g, 44% yield).

Synthesis of 12,13-bis(2-butyloctyl)-3,9-bis(10-methoxydecyl)-12,13-dihydro-[1,2,5]thiadiazolo[3,4-e]thieno[2'',3'':4',5']thieno[2',3':4,5]pyrrolo[3,2-g]thieno[2',3':4,5]thieno[3,2-b]indole-2,10-dicarbaldehyde (9): Under a nitrogen atmosphere, $POCl_3$ (1.2 g, 8.0 mmol) was slowly added to dry DMF (50 mL) in a two-necked flask. The mixture was stirred at room temperature for 0.5 h, after which a solution of compound 8 (670 mg, 0.60 mmol) in dry CH_2Cl_2 (20 mL) was added dropwise. The resulting reaction mixture was stirred at 60°C for 12 h. Upon completion, the mixture was slowly poured into a saturated aqueous $NaHCO_3$ solution (150 mL) and extracted with ethyl acetate. The combined organic layers were washed with saturated aqueous NaCl, dried over anhydrous Na_2SO_4, filtered, and concentrated under reduced pressure. Purification by column chromatography on silica gel, eluting with a gradient of ethyl acetate in petroleum ether, afforded the desired product 9 as an orange solid (534 mg, 73% yield).

Synthesis of 2,2'-((2Z,2'Z)-((12,13-bis(2-butyloctyl)-3,9-bis(10-methoxydecyl)-12,13-dihydro-[1,2,5]thiadiazolo[3,4-e]thieno[2'',3'':4',5']thieno[2',3':4,5]pyrrolo[3,2-g]thieno[2',3':4,5]thieno[3,2-b]indole-2,10-diyl)bis(methaneylylidene))bis(5,6-difluoro-3-oxo-2,3-dihydro-1H-indene-2,1-diylidene))dimalononitrile (2OM): To a two-necked flask charged with compound 6 (352 mg, 0.30 mmol) under a nitrogen atmosphere, 2-(5,6-difluoro-3-oxo-2,3-dihydro-1H-inden-1-ylidene)malononitrile (207 mg, 0.90 mmol), $CHCl_3$ (30 mL), and pyridine (1 mL) were added sequentially. The reaction mixture was stirred at 60°C for 12 h. After completion, as determined by TLC analysis, the solvent was removed under reduced pressure. The residue was purified by column chromatography on silica gel, eluting with dichloromethane/methanol, to afford compound 2OM as a dark solid (254 mg, 53% yield). ^{1}H NMR (400 MHz, Chloroform-*d*) δ 9.17 (s, 2H), 8.58 (dd, *J* = 10.0, 6.5 Hz, 2H), 7.70 (t, *J* = 7.2 Hz, 2H), 4.83 – 4.70 (m, 4H), 3.44 – 3.28 (m, 10H), 3.24 (t, *J* = 8.0 Hz, 4H), 2.17 – 2.08 (m, 2H), 1.92 – 1.83 (m, 4H), 1.44 – 0.58 (m, 72H). ^{13}C NMR (101 MHz, Chloroform-*d*) δ 186.11, 158.83, 153.85, 147.49, 145.17, 137.68, 136.01, 135.24, 134.49, 134.18, 133.28, 119.97, 114.97, 114.86, 114.58, 113.57, 112.33, 72.97, 68.71, 58.55, 55.71, 39.21, 31.59, 31.24, 30.52, 30.40, 29.85, 29.67, 29.59, 29.49, 29.45, 29.40, 28.09, 27.90, 26.14, 25.43, 25.23, 22.86, 22.81, 22.49, 22.47, 14.04, 14.02, 13.80, 13.76.

2 Experimental Section

2.1 Characterization of photovoltaic materials

UV–vis absorption spectra were recorded on a Shimadzu UV-3600 spectrophotometer over the range of 300–1000 nm, with correction for quartz substrate absorption.

Cyclic voltammetry (CV) measurements were performed using a CHI660E electrochemical workstation, employing a three-electrode system consisting of a glassy carbon working electrode, a platinum wire counter electrode, and a saturated calomel reference electrode (SCE). All potentials were referenced to the ferrocene/ferrocenium (Fc/Fc^+) redox couple, which was measured under the same conditions and assigned a potential of −4.80 eV.

2.2 Device fabrication and characterization

The photovoltaic devices were fabricated in an inverted architecture: ITO/AZO/active layer/2PACz/MoO_3/Ag. Indium tin oxide (ITO)-coated glass substrates were sequentially cleaned by sonication in detergent, deionized water, and anhydrous ethanol (each for 15 min), followed by drying in an oven at 60°C overnight. Prior to use, the substrates were treated with oxygen plasma for 5 min. A solution of aluminum-doped zinc oxide (AZO) was then spin-coated onto the ITO surface and subsequently annealed on a hot plate at 150 °C in ambient air for 15 min. The substrates were then transferred into a nitrogen-filled glovebox for subsequent processing. The active layer solution was prepared by dissolving the donor and acceptor materials in a 1:1.2 weight ratio (4.0 mg mL^{-1} : 4.8 mg mL^{-1}) in a mixed solvent of carbon disulfide and *o*-xylene (volume ratio = 1:1). The solution was stirred at 70 °C for 2 h under nitrogen atmosphere. The active layer was spin-coated at 2200 rpm onto preheated AZO-coated substrates to form a ~100 nm thick film. Subsequently, a dilute solution of 2PACz in ethanol was spin-coated at 3000 rpm onto the active layer and thermally annealed at 100 °C for 10 min. Finally, MoO_3 (10 nm) and Ag (100 nm) were successively deposited through a shadow mask by thermal evaporation under high vacuum (pressure ~1×10^{-7} mbar) to form the top electrode. The effective device area was defined as 0.04 cm^2 using a metal aperture mask with non-reflective coating to ensure accurate photovoltaic parameter measurement. Current density-voltage (*J–V*) characteristics were measured using a computer-controlled Keithley 2400 source meter under simulated AM 1.5G solar irradiation (100 mW cm^{-2}, 1 sun intensity) from a solar simulator (Enlitech SS-F5, Taiwan). The light intensity was calibrated using a certified reference silicon solar cell (traceable to the China General Certification Center) prior to device testing. External quantum efficiency (EQE) spectra were recorded using a QE-R3011 system

(Enlitech, Taiwan) under zero-bias conditions.

2.3 Space charge limited current (SCLC) measurements

The SCLC model formula is defined by Equation S1.

$$J = \frac{9}{8}\varepsilon_0\varepsilon_r\mu V^2 d^{-3} \#(S1)$$

Where J is current density, ε_0 is the permittivity of free space, ε_r is the relative permittivity of the material, μ is the zero-field mobility, and d is the thickness of films. The V is effective voltage calculated by the equation: $V=V_{appl}-V_{bi}-V_s$, where V appl is the applied voltage, V_{bi} is the built-in voltage, and V_s is the voltage drop of the substrate series resistance.

2.4 Morphology measurements

Atomic force microscopy (AFM): AFM measurements were performed in tapping mode using a Digital Instruments Multimode Nanoscope III atomic force microscope.

Grazing-Incidence Wide-Angle and Small-Angle X-ray Scattering (GIWAXS/GISAXS): GIWAXS and GISAXS measurements were conducted on a laboratory-scale Xeuss 2.0 SAXS/WAXS system (Xenocs) equipped with a Cu Kα X-ray source (λ = 1.54 Å, 8.05 keV) and a Pilatus3R 300K hybrid photon-counting detector. The incident X-ray beam angle was set to 0.2° for all measurements.

Contact Angle and Surface Energy Measurements: Contact angles were measured using a sessile drop method on an OCA40 Micro system. Deionized water and ethylene glycol were used as probe liquids. Surface energy was calculated according to the equation-of-state method. The surface energy (γ) of neat films of D18, Y6-BO, 1OM and 2OM were determined using the Owens-Wendt model.[1] The approach is based on the following equations:

$$\gamma_L(1 + cos\theta) = 2\sqrt{\gamma_S^d\gamma_L^d} + 2\sqrt{\gamma_S^p\gamma_L^p}$$

$$\gamma_S = \gamma_S^d + \gamma_S^p$$

where γ_L^d and γ_L^p are the dispersive and polar components of the liquid surface tension, respectively, and γ_S^d and γ_S^p are the corresponding dispersive and polar components of the solid surface energy. The surface tension components for water and ethylene glycol were taken from the literature.[2] The Flory-Huggins interaction parameters (χ) between donor and acceptor were estimated using the relation: $\chi_{DA} = K\left(\sqrt{\gamma_D} - \sqrt{\gamma_A}\right)^2$, where K is a positive constant, γ_D and γ_A represent the total surface energies of the donor and acceptor materials, respectively.

2.5 Spectroscopic measurements

Transient photocurrent (TPC) and transient photovoltage (TPV) measurements: TPC and TPV measurements were performed using 500 nm laser pulses generated by an optical parametric amplifier (TOPAS-Prime), which was pumped by a mode-locked Ti:sapphire oscillator seeded regenerative amplifier system (Spitfire Ace, Spectra Physics) operating at 800 nm with a pulse energy of 1.3 mJ and a repetition rate of 1 kHz. The laser pulses had a duration of approximately 120 fs and were attenuated to low excitation fluences to ensure operation under linear-response conditions. For TPC measurements, the device was held under short-circuit conditions by connecting both terminals through a 50 Ω resistor to ground, effectively mimicking a short circuit and allowing for efficient charge extraction. The decay of the photocurrent under zero applied bias is primarily governed by carrier sweep-out rather than recombination. Therefore, the TPC signal reflects the charge extraction dynamics, with recombination losses being negligible under short-circuit conditions. The charge extraction time was determined by fitting the TPC decay trace to a single-exponential function: $\delta I=Aexp(t/T)$, where A is a constant that fits the peak height, t is time, and T is the charge extraction time. For TPV measurements, the device was held under open-circuit conditions, with a DC bias applied via a power supply connected in parallel to the input of a digital oscilloscope to maintain the operating point at open circuit. The photovoltage decay kinetics were monitored following a small perturbation, and all devices exhibited mono-exponential decay behavior, described by: $\delta V=Aexp(-t/T)$, where t is the time, and T is the charge carrier lifetime.

***Capacitance-frequency (C-ω) and Mott-Schottky measurements*:** *C-ω* measurements were performed using the PAIOS advanced optoelectronic characterization platform, which integrates comprehensive testing capabilities for solar cells and organic light-emitting diodes (OLEDs). The *C-ω* measurements were carried out under dark conditions over a frequency range of 1 Hz to 10 MHz. Mott-Schottky analysis was conducted under dark conditions by sweeping the DC bias voltage from −3 V to 2 V. The resulting capacitance data were analyzed according to the Mott–Schottky equation (Equation S2):

$$\frac{1}{C^2}=\frac{2(V_{bi}-V)}{A^2 q\varepsilon_0\varepsilon_r N}\#(S2)$$

Where C is the capacitance value, V is the applied voltage, A is the device area, q is the elementary charge, ε_r is the relative dielectric constant, ε_0 is the vacuum permit-tivity, and N is the charge carrier density.

***Photo-CELIV measurements*:** Photo-CELIV measurements were performed using the PAIOS

optoelectronic characterization system under varying light intensities. The measurements were conducted with a linear voltage ramp of 200 V s^{-1}, a delay time of 0 s, an offset voltage of 0 V, and a light pulse duration of 100 μs, synchronized with the voltage sweep to ensure consistent photoexcitation conditions.

femtosecond transient absorption (TA) measurement: the fs-TA spectra in the visible and near infrared range were obtained using a broadband pump-probe transient absorption spectrometer (Helios Fire, Ultrafast Systems), employing an amplified 1030 nm laser (Pharos, Light Conversion, 200 fs, 200 μJ, 1 kHz). The fundamental laser was tuned to 420 nm with an optical parametric amplifier (Orpheus-F, Light Conversion) and used as the excitation. Fiber-coupled alignment-free spectrometer with a 1024 pixel CMOS sensor (spectral response: 200-1000 nm) is used as visible signals detector. Fiber-coupled alignment-free spectrometer with a 256 pixel InGaAs sensor (spectral response: 800−1600 nm) is used as NIR detector. All TA measurements were performed at 293 K. Data analysis was performed based on Surface Xplorer software package.

3. Supplementary Figures and Tables

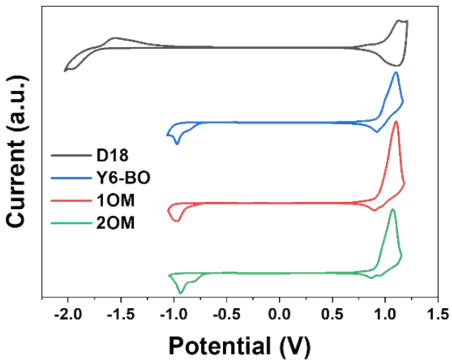

Fig. S1. The CV curves of D18, Y6-BO, 1OM, and 2OM.

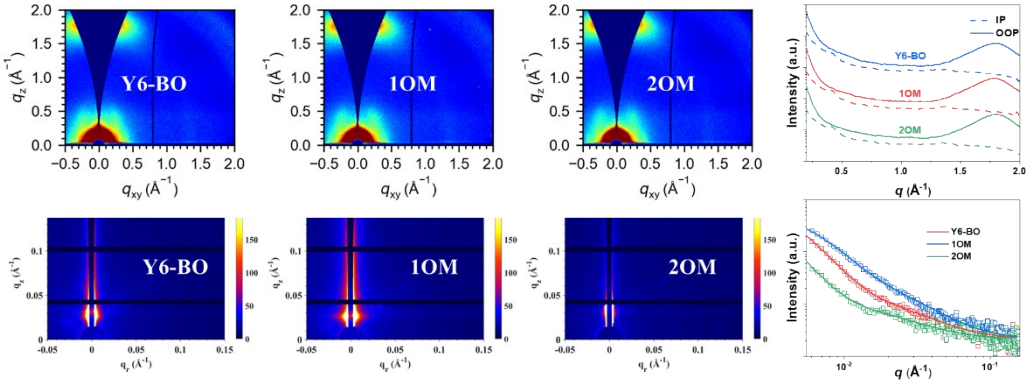

Fig. S2. 2D GIWAXS and 2D GISAXS images and corresponding 1D profiles for Y6-BO, 1OM, and 2OM neat films.

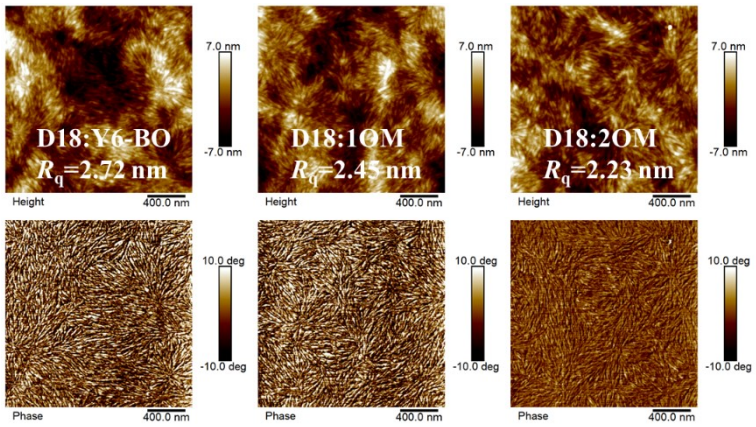

Fig. S3. AFM height and phase images of the D18:Y6-BO, D18:1OM, and D18:2OM blend films.

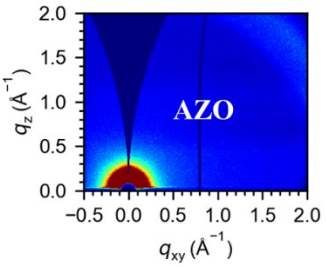

Fig. S4. 2D GIWAXS images of AZO film.

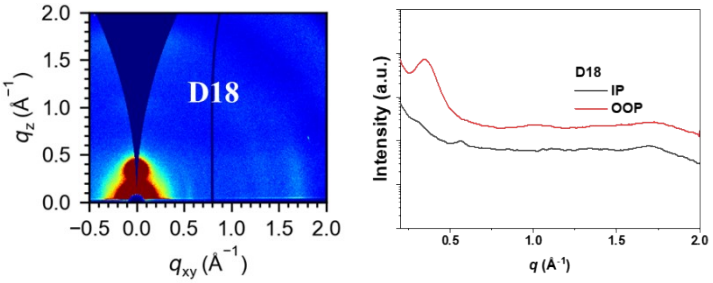

Fig. S5. 2D GIWAXS and corresponding 1D profiles for D18 neat films.

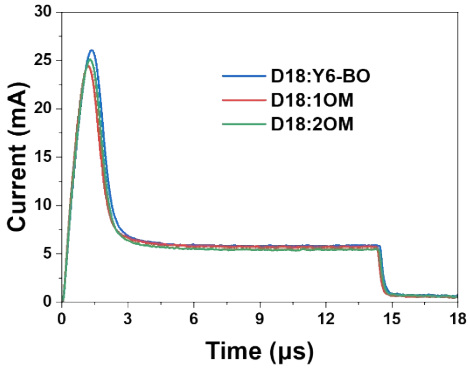

Fig. S6. Photo-CELIV curves for D18:Y6-BO-, D18:1OM-, and D18:2OM-based OPVs.

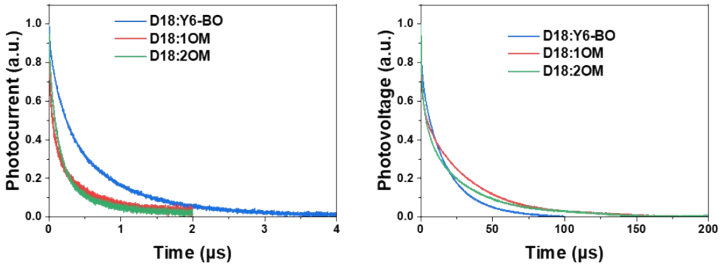

Fig. S7. TPC and TPV curves for D18:Y6-BO-, D18:1OM-, and D18:2OM-based OPVs.

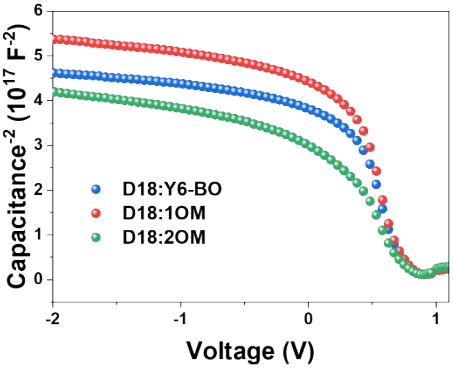

Fig. S8. Mott-Schottky curves of D18:Y6-BO-, D18:1OM-, and D18:2OM-based devices.

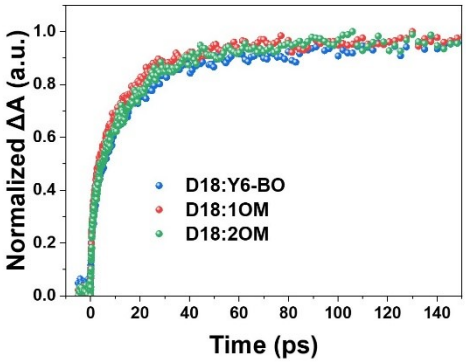

Fig. S9. The TA kinetics at 595 nm of D18:Y6BO, D18:1OM, and D18:2OM blend film, excited at 750 nm.

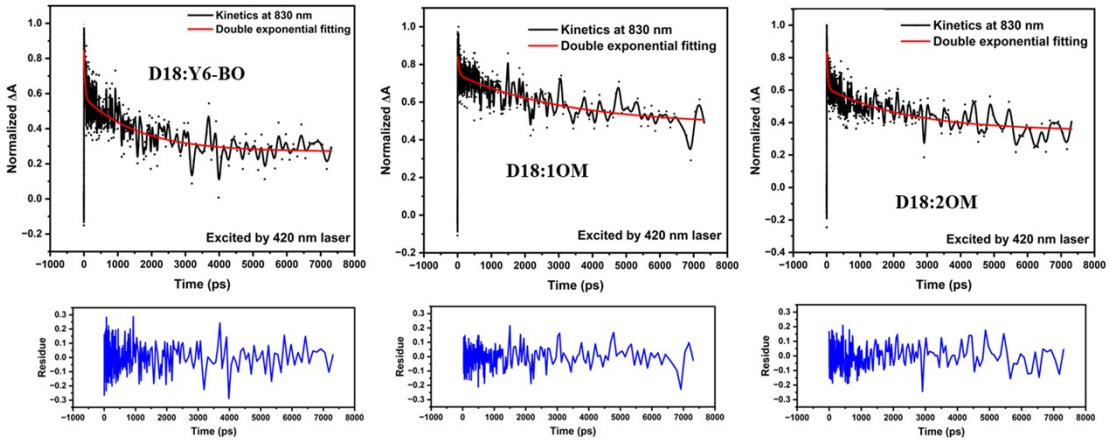

Fig. S10. The extracted kinetics, double exponential fitting, and fitting residue at 830 nm of D18:Y6BO, D18:1OM, and D18:2OM, respectively. The samples are excited by 420 nm laser.

Table S1. Molecular packing parameters of corresponding films.

Sample	Peak	Peak location ($Å^{-1}$)	π-π stacking distance (Å)	FWHM ($Å^{-1}$)	Crystal coherence length (Å)
Y6BO	(100) In IP	0.386	\	\	\
	(010) In OOP	1.791	3.51	0.282	19.7
1OM	(100) In IP	0.386	\	\	\
	(010) In OOP	1.797	3.50	0.269	20.7

2OM	(100) In IP	0.393	\	\	\
	(010) In OOP	1.800	3.49	0.261	21.3
D18	(100) In OOP	0.345	\	\	\
D18:Y6BO	(100) In IP	0.300	\	\	\
	(010) In OOP	0.471/1.746	13.33/3.60	0.114/0.227	49.6/24.9
D18:1OM	(100) In IP	0.304	\	\	\
	(010) In OOP	0.512/1.756	12.27/3.58	0.057/0.217	99.2/26.0
D18:2OM	(100) In IP	0.307	\	\	\
	(010) In OOP	1.772	3.54	0.212	26.7

Table S2. Summaries of fitting results.

blend	A_1	τ_1 (ps)	A_2	τ_2 (ps)	$\tau_{ave.}(ps)$
D18:Y6-BO	0.20	28.55	0.31	1621.46	1596.74
D18:1OM	0.10	43.42	0.27	3235.09	3219.02
D18:2OM	0.24	32.77	0.26	2481.36	2452.76

References

1 D. K. Owens, R. C. Wendt, *J. Appl. Polym. Sci.* 1969, **13**, 1741.

2 A. Kozbial, Z. Li, C. Conaway, R. McGinley, S. Dhingra, V. Vahdat, F. Zhou, B. D'Urso, H. Liu, L. Li, *Langmuir* 2014, **30**, 8598.